# Ferromagnetism in transparent thin films of MgO

C. Martínez-Boubeta,[1] J. I. Beltrán,[2] Ll. Balcells,[3] Z. Konstantinović,[3] S. Valencia,[4] D. Schmitz,[4] J. Arbiol,[3,5] S. Estrade,[1] J. Cornil,[2] and B. Martínez[3,*]

[1]*IN²UB and Departament d'Electrònica, Universitat de Barcelona, 08028 Barcelona, Spain*

[2]*Laboratory for Chemistry of Novel Materials, Université de Mons-Hainaut, 7000 Mons, Belgium*

[3]*Instituto de Ciencia de Materiales de Barcelona (ICMAB), CSIC, Campus UAB, 08193 Bellaterra, Spain*

[4]*Helmholtz-Zentrum Berlin für Materialien und Energie, Albert-Einstein-Str. 15, 12489 Berlin, Germany*

[5]*Institut Català de Recerca i Estudis Avançats (ICREA), Barcelona, Spain*

(Received 11 January 2010; revised manuscript received 1 June 2010; published 8 July 2010)

We show both theoretical and experimental evidences of the appearance of ferromagnetism in MgO thin films. First-principles calculations allow predicting the possibility of the formation of a local moment in MgO, provided the existence of Mg vacancies which create holes on acceptor levels near the O $2p$-dominated valence band. Magnetic measurements evidence of the existence of room-temperature ferromagnetism in MgO thin films. High-resolution transmission electron microscopy demonstrates the existence of cation vacancies in our samples. Finally, by applying the element specificity of the x-ray magnetic circular dichroism technique, we also demonstrate that the magnetic moments of the system arise from the spin polarization of the $2p$ electrons of oxygen atoms surrounding Mg vacancies.

DOI: 10.1103/PhysRevB.82.024405 PACS number(s): 75.70.−i, 61.72.Bb, 68.37.Og, 71.15.Mb

## I. INTRODUCTION

It is expected that combining spin and charge degrees of freedom in the same material will allow a straightforward implementation of spintronics devices with new and enhanced functionalities. In pursuit of this paradigm a huge research effort has been concentrated in the recent years on the so-called diluted magnetic semiconductors, including wide band-gap nitrides and oxides.[1] Accordingly, the unexpected finding that $p$ bands can spontaneously polarize giving a ferromagnetic (FM) state in materials as diverse as ZnO, $Al_2O_3$, or graphite, just to mention a few (Refs. 2–7) opened a new direction in the research field of diluted magnets. However, in spite of the vast amount of work already done the intrinsic nature of this unexpected FM is still obscure, and a clear connection between microstructure and magnetic behavior is still lacking.[8] One feature in common in all these reports is that structural defects (interfaces, grain boundaries, dislocations, vacancies,…) that are profusely present in the studied materials, may well play a leading role on the appearance of the FM ordering. Thus, microstructural features have become of utmost importance for the investigation of unconventional magnetic properties and, as a consequence, have been the subject of intense research.[9–11] Noteworthy, there is an increasing awareness that further progress in the development of spin-dependent devices based on diluted magnetic semiconductors will require the ability to control the incorporation and distribution of impurities.[12]

On the other hand, most of the theoretical studies predicting the existence of unexpected magnetic moments (mm) are based on the density-functional theory (DFT) using local or semilocal exchange-correlation (XC) functionals.[11,13,14] However, these theoretical predictions have been questioned by some authors[15] arguing that calculations based on local or semilocal functionals are unable to properly capture Jahn-Teller distortions due to the fact that those functionals do not predict the correct polaronic localization. These limitations fully apply for materials with narrow band gap, as in the case of ZnO,[15] in which the hole-wave function is incorrectly distributed over all four O neighbors, thus incorrectly predicting a delocalized degenerated ground state. On the other hand, in wide band-gap oxides such as MgO, evidences for a localized model appear to contradict calculations and experiments which have been interpreted as justifying the delocalized ground state. In the excited state it is indeed likely that the holes are delocalized.[16–18] Still, the question of whether localization enhances or reduces magnetic correlation is central to the physics of diluted magnetic semiconductors.[19]

MgO is perhaps one of the best characterized metal-oxide materials in terms of defects and impurities and often considered a model oxide system[20] but also an important material with many applications. For instance, a magnesia protective layer is routinely used on an ac-type plasma display panel since it provides excellent ion bombardment protection while being high transparent to visible radiation.[21] Interest is heightened by the fact that alkaline-earth oxides are highly refractory insulators also playing an important role in heterogeneous catalysis.[22] Consequently, defective sites in MgO have been the subject of considerable experimental and theoretical attentions over the last decades. They may introduce new electronic states, giving rise to a variety of optical and electrical conductivity phenomena.[23,24] For example, it is suggested that oxygen vacancies in MgO might improve the energy conversion efficiency in solar cells[25] and open the way for tunable solid-state lasers.[26] Additionally, crystalline MgO barriers for spintronics have generated a great deal of interest for the last 10 years.[27] In this regard, the exploitation of spin selective ferromagnetic insulators would be of great importance.[28] It is envisaged that ferromagnetism in transparent oxides would allow for new "see-through" spin photonic devices.

MgO displays a rocksalt structure with both Mg and O atoms octahedrically coordinated, making pure MgO a diamagnetic material. The magnetic properties of MgO were extensively studied by Pacchioni[18] and Noguera and

 

co-workers[29] suggesting the appearance of magnetic moments in the local environment of low coordinated O atoms at the surface. Noteworthy, theoretical studies using quantum Monte Carlo methods suggest the existence of stable moments in N-doped MgO.[30] Moreover, a recent report by Peng *et al.*[11] suggest that spontaneous magnetization in nitrides and oxides are an intrinsic property of these first-row semiconductors due to the localized nature of $2p$ states of O and N atoms.

In this work we tackle this issue by using first-principles calculations based on the generalized gradient approximation (GGA), which even being not the highest theory level is providing a good comparison to our experimental measurements. In our previous work we have shown the possibility of inducing spin polarization at the MgO surface[31] and, we have also reported strong evidences of the existence of intrinsic ferromagnetism at room temperature in MgO nanocrystals with cation vacancies.[32] Here, we have extended our theoretical studies to demonstrate the possibility of inducing magnetic moments in Mg-defective MgO. This fact is experimentally confirmed by x-ray magnetic circular dichroism (XMCD) that evidences that magnetic moments in MgO thin films with Mg vacancies, whose existence has been proved by using high-resolution transmission electron microscopy (HRTEM), arise from the spin polarization of the $2p$ electrons of oxygen atoms surrounding Mg vacancies. Finally, conventional magnetometry methodologies demonstrate the existence of room-temperature ferromagnetism in these Mg-defective MgO thin films.

## II. THEORETICAL APPROACH

Our first-principles calculations on MgO have been performed within the DFT using the SIESTA code.[33] We employed the Perdew-Burke-Ernzerhof flavor within the GGA as the XC energy functional.[34] The employed real-space grid has an equivalent cutoff larger than 300 Ryd and relaxation was performed till atomic forces are lesser than 0.05 eV/Å. For the largest studied supercell no quantitative convergence was obtained for the former parameter, see below in the discussion. More details about the settings of the calculations can be found elsewhere.[32] We have analyzed the role of both O and Mg vacancies in the MgO structure and we found that only the latter triggers the appearance of magnetic moments. Similar dependence on cation vacancies has been already established several years ago by Elfimov *et al.*[35] in CaO. In this work we will analyze the role of Mg vacancies, which are to be referred as $V_{Mg}$. For that reason, we have used a periodic boundary conditions code in which the vacancies are homogeneously distributed in a so-called periodic vacancy network created by a repeating unit, called supercell. Each supercell includes only one $V_{Mg}$ and is created by three vectors according to different lattices such as, simple cubic (sc), face-centered cubic (fcc), and body-centered cubic (bcc). For the sake of clarity these vectors are depicted in Fig. 1(a) within a supercell which is $2\times2\times2$ times the MgO unit cell. The number of $V_{Mg}$-$V_{Mg}$ nearest neighbors (NNs) varies with the nature of the vectors, from six in sc, eight in bcc to 12 in fcc. For each of these lattices the length of the

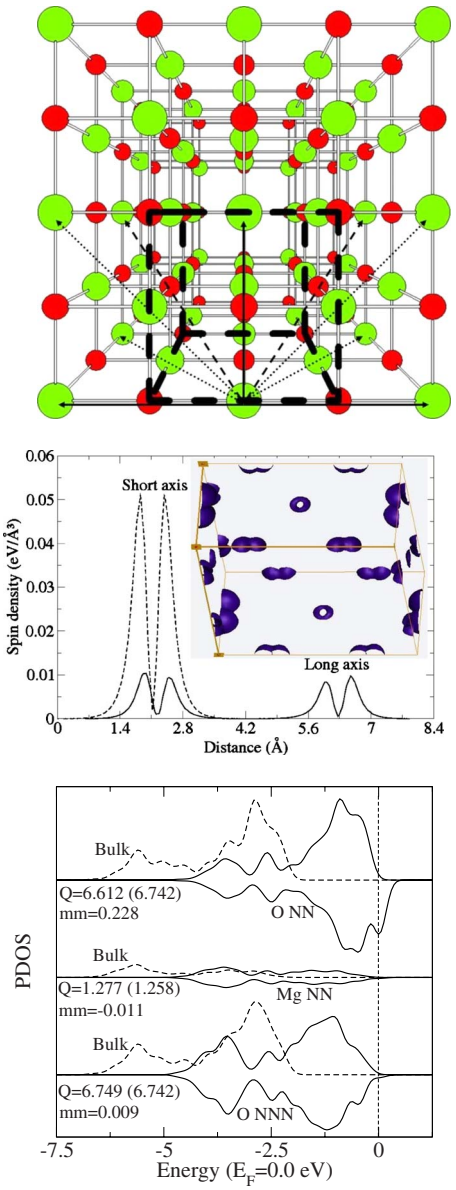


FIG. 1. (Color online) Theoretical results on the magnetization dependence on cation vacancies. (a) Perspective view of the atomic layout in a $2\times2\times2$ times MgO unit cell, or sc 64 atoms, with the unit cell highlighted in bold dashed lines. The green (big) and red (small) circles correspond to Mg and O atoms, respectively. The vectors characterizing the different lattices, used for the construction of the periodic $V_{Mg}$ network, are depicted by lines: continuous for sc, dashed for bcc, and dotted for fcc. (b) Spin density for the sc 32 atoms supercell along the two different axis with short (4.25 Å) and long (8.50 Å) lengths. The lobe shape distribution resembles the $2p$ orbitals of the O atom. Inset: spin density plot at a constant value of $1.2\times10^{-3}$ electrons/(Å$^3$) for the sc 32 atoms supercell with one $V_{Mg}$ located in the vertexes of the prism. (c) PDOS on the atoms of the fcc 54 atoms supercell lying within 3.7 Å from the $V_{Mg}$ are shown by a continuous line. That PDOS is spin decomposed in major (positive) and minor (negative) components and is compared to the nonspin decomposed PDOS of the equivalent atoms in MgO absent of $V_{Mg}$ (dashed line). The Mulliken population ($Q$) in $|e|$ and the magnetic moment (mm) in Bohr magneton of the selected atoms are also given compared to the bulk value in between parentheses.

TABLE I. Spin polarization density for the different supercell configurations with one Mg vacancy. The number of $V_{Mg}$-$V_{Mg}$ NN is influenced by both the lattice type and the dimension of the periodic $V_{Mg}$ network. $V_{Mg}$-$V_{Mg}$ distances, the volume, and the number of atoms per supercell are also indicated. A range in the magnetic-moment values have been included between brackets for the 128 atoms supercell corresponding to values of 400 and 500 Ryd in the "mesh cutoff" code parameter, which indicates uncertainty for the largest calculated supercell.

| Lattice | $V_{Mg}$ network | NN | Shortest‖largest $V_{Mg}$-$V_{Mg}$ distance (Å) | Volume(Å$^3$)‖atoms per supercell | Spin polarization ($\mu_B$/supercell)‖(emu/cm$^3$) |
|---|---|---|---|---|---|
| fcc | 3D | 12 | 6.10 | 159.6‖16 | 1.94‖113 |
| | 3D | 12 | 9.13 | 533.8‖54 | 1.64‖28 |
| | 3D | 12 | 12.03 | 1227.0‖128 | 0.00(0.02–0.40)‖0(0.19–2.95) |
| bcc | 3D | 8 | 7.45 | 316.8‖32 | 1.45‖42 |
| sc | 3D | 6 | 4.23 | 75.9‖8 | 2.00‖244 |
| | 2D | 4 | 4.25‖8.57 | 154.7‖16 | 1.96‖117 |
| | 1D | 2 | 4.25‖8.55 | 310.6‖32 | 1.64‖49 |
| | 3D | 6 | 8.52 | 618.8‖64 | 0.14‖2 |

vectors is varied, and so the volume per vacancy, so that we can correlate the magnetization to the density of vacancies and also vary $V_{Mg}$ to $V_{Mg}$ distances to evaluate the effect on the magnetization, as shown in Fig. 1(b). The main results concerning all supercell structures and magnetization values are summarized in Table I. All entries in the table corresponds to homogeneous periodic three-dimensional (3D) vacancy network except for the sc lattice in which the dimension (NN) of the periodic $V_{Mg}$ network has been reduced from 3D (6) to two dimensional (2D) (4) and one dimensional (1D) (2), respectively. It is worth mentioning that our calculations indicate that in all the supercells analyzed FM interactions are more stable than antiferromagnetic ones. An important result from Table I is that the magnetic moment per cell is approximately constant and equal to 2 $\mu_B$, which corresponds to the number of holes generated by a $V_{Mg}$, for concentrations up to one $V_{Mg}$ each 16 atoms. Therefore, since each supercell contains one $V_{Mg}$, the magnetization per volume decreases almost linearly by increasing the supercell volume. For supercells with more than 16 atoms, there is also an important additional decrease in the magnetization per supercell since the perturbation of the electronic structure of distant O atoms due to the presence of the $V_{Mg}$ is vanishing small so, their contribution to the magnetization is drastically reduced. However in the largest supercell case the value is not totally converged with respect to the code parameters: mesh cutoff and the atomic forces, therefore the calculated magnetic moment has to be considered more qualitatively than quantitatively. The range of magnetic-moment values obtained for more restricting conditions, than those specified in the theoretical approach section, are included between brackets in Table I for the 128 atoms supercell.

To gain a deeper insight into the nature of the magnetic moments generated we plot in the inset of Fig. 1(b) the distribution of the polarization density for the sc 32 atoms supercell. The $V_{Mg}$ is located at the corners of the prism and so two different $V_{Mg}$-$V_{Mg}$ distances can be considered as corresponding to the long and the short axes. Along the short axis the value of the polarization density reaches a maximum around five times larger than that along the long axis, as illustrated in Fig. 1(b). The location of these maxima corresponds to the O NN to the $V_{Mg}$ (see inset) and whose polarization density distribution presents a lobe shape resembling that of the $2p$ O orbitals, like it has been previously stated by others.[11,18,31,36] These conclusions are also valid for other supercells although the respective calculations are not so easy to depict.

In order to assign to some entity the onset in the magnetic moment, which is induced by the presence of the $V_{Mg}$, we present in Fig. 1(c) the projection of the density of states (PDOS) on the atoms that are closer than 3.7 Å to the $V_{Mg}$ of a fcc 54 atoms supercell. It can be seen in Fig. 1(c) that the magnetism is mostly created at O atoms NN to the $V_{Mg}$, which totally accounts for 1.37 $\mu_B$ while for further atoms such as Mg NN and O next NN to the $V_{Mg}$ the magnetism is strongly reduced to −0.13 $\mu_B$ and 0.10 $\mu_B$, respectively. In addition to the large difference between the majority- and the minority-spin contributions for the O atoms that carry most of the magnetism, in good agreement with Gao *et al.*,[10] a valence-band shift of about 2 eV with respect to the O PDOS corresponding to bulk is obtained. This valence-band shift is related to a different electronic distribution in the presence of $V_{Mg}$. The appearance of the spin polarization is, on the other hand, related to the reduction in the Mulliken population at the O atoms. When a magnetic signal is generated, the electronic charge (calculated by a Mulliken population analysis) on the O atoms NN to the $V_{Mg}$ is reduced by more than 5% in sc eight atoms supercell and by around 2% in supercells of around 60 atoms with respect to the charge of O in the MgO bulk. A similar discussion of the onset of magnetism in oxides due to the charge distribution in the O atoms has been previously reported.[31]

Therefore, our theoretical study indicates that the polarization of $2p$ O orbitals, due to the modification of the electronic charge distribution because of the presence of $V_{Mg}$, triggers the appearance of magnetic moments. It turns out that magnetization strongly depends on the $V_{Mg}$ concentration and slightly on $V_{Mg}$ coordination. From Table I, the largest cell for which the magnetic moment is not vanishingly

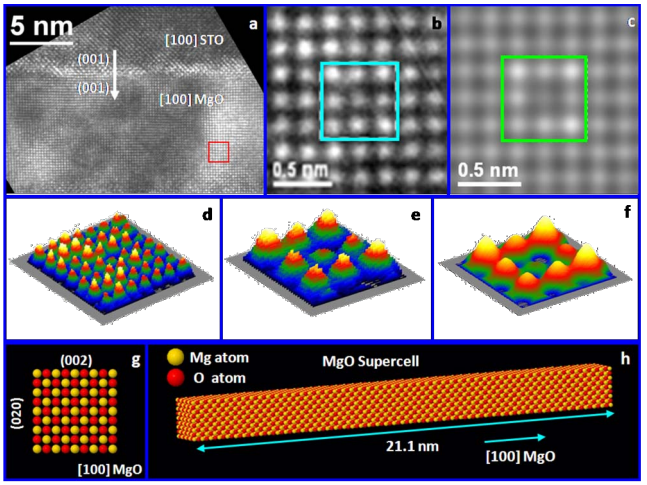


FIG. 2. (Color online) (a) HRTEM general view of the MgO layer (10 nm) grown on the STO substrate. Both layers grow along their respective [001] axis. (b) HRTEM detail of the MgO layer corresponding to the red squared area in (a). (c) HRTEM computer simulation of the same area in (b), simulation parameters: beam energy=200 kV, Cs=0.5, Cc=1.1, energy spread=0.8 eV, defocus=−53.4 nm, and thickness 21.1 nm. (d) 3D intensity map of the experimental HRTEM image shown in (b). (e) 3D intensity map of the nine central atomic columns squared (cyan) in the experimental detail (b). (f) 3D intensity map of the nine central atomic columns squared (green) in the HRTEM computer simulation in (c). (g) Frontal view of the MgO supercell used to obtain the simulated image in (c). (h) Side view of the same supercell in (g).

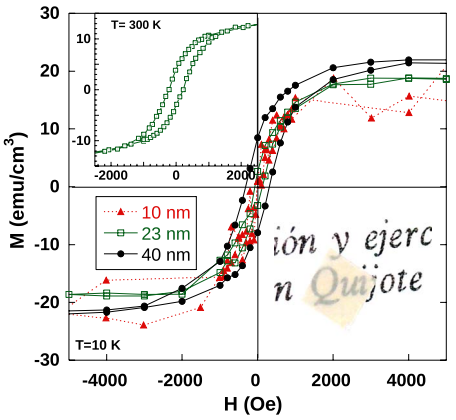


FIG. 3. (Color online) Hysteresis $M(H)$ curves of MgO(001) films of different thicknesses on $SrTiO_3$ taken at room temperature and 10 K. Magnetic field was applied parallel to the film surface. The films are transparent enough in the visible region to make the background text readable (inset on the right).

small corresponds to a concentration of vacancies of $\sim 1.9 \times 10^{-3} V_{Mg}/Å^{-3}$ which, in turns, corresponds to a magnetization of $\sim 28$ emu/cm$^3$. These results also suggest that magnetization would increase by increasing $V_{Mg}$ concentration.

## III. EXPERIMENTAL RESULTS

In the previous section we have shown that theoretical calculations indicate that the modification of the electronic charge distribution, because of the presence of $V_{Mg}$, may trigger the appearance of magnetic moments in MgO. To experimentally test the feasibility of having room-temperature FM in defective MgO we have prepared MgO thin films by using the sputtering technique in an excess of oxygen atmosphere (0.25 torr) at high temperature (1073 K) to promote the generation of Mg vacancies.[37,38] We have used (001) oriented $SrTiO_3$ (STO) substrates treated before deposition to select a unique atomic termination and a MgO monocrystalline target.[39]

### A. Structural characterization

The microstructural features of the films were checked at atomic level, looking for evidences of the existence of $V_{Mg}$, by HRTEM using a Jeol 2010F field-emission gun microscope. Figure 2(a) displays a HRTEM general view of a 10-nm-thick layer of MgO grown on STO substrate. As depicted, both materials (substrate and layer) grow along their respective [001] axis, with the $(001)[100]_{MgO}//(001)[100]_{STO}$ epitaxial relationship. In Fig. 2(b) we show a HRTEM detail of the MgO layer corresponding to the highlighted area in Fig. 2(a). At a first glance we noticed important changes in the projected intensity of the different atomic columns. A 3D intensity map of the experimental HRTEM image shown in Fig. 2(b) is depicted in Fig. 2(d). As in the whole area the background intensity average is kept constant, in these conditions the differences in atomic column intensity could not be attributed to thickness changes. An intensity map of the nine central atomic columns squared in Fig. 2(b) is displayed in Fig. 2(e), revealing clear changes in intensity in every column. As in previous analysis,[40] these data were fitted by using atomic modeling and image simulation. Once the preliminary 3D atomic model was designed as shown in Figs. 2(g) and 2(h), the effect of introducing Mg vacancies in a $(100)_{MgO}$ column on the HRTEM simulated micrographs was analyzed. As illustrated in Fig. 2(f), the intensities observed in Fig. 2(e) are well reproduced by the model. Therefore, these data strongly indicate the existence of about $2 \times 10^{-3} V_{Mg}/Å^3$ within the MgO matrix. Such a vacancy concentration $\sim 10^{21}$/cm$^3$, although high, is not unusual in MgO.[24,41] For the sake of comparison, in virgin MgO crystals the concentration of $V$-type centers is typically $\sim 10^{18}$/cm$^3$.[42] It should be mentioned that in our case the deposition of atoms proceeded at temperatures well above the Mg melting point ($\sim$923 K). Thus, it is very likely that the re-evaporation of Mg when arriving at the substrate, together with the excess oxygen pressure, might help to stabilize the Mg vacancies.

### B. Magnetic characterization

The magnetic properties of MgO thin films were measured using both superconducting quantum interference device and vibrating sample magnetometers from Quantum Design for reproducibility purposes. Magnetization measurements depicted in Fig. 3 demonstrate the existence of room-temperature ferromagnetic ordering, almost thickness independent, in MgO films. Data were corrected for substrate

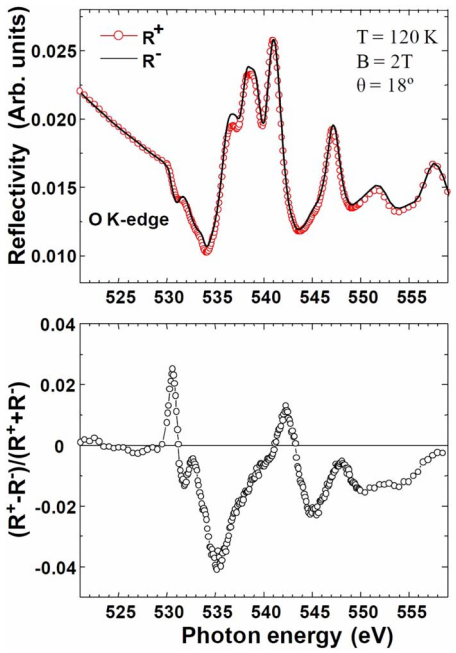


FIG. 4. (Color online) Top: O $K$ edge x-ray scattering structure. Bottom: XRMS spectra collected at 120 K. The sample was magnetically saturated applying a magnetic field of 2 T nearly parallel to its surface plane. The angle of incidence of the radiation on the sample, with respect to the surface plane was $\theta_i = 18°$. The degree of polarization of the incoming radiation was $P = 0.9$. Spectra were collected by a photodiode set at angle $2\theta_i$.

contribution, leading to a saturation magnetization at low temperature ($T = 10$ K) of $M_s \sim 20-30$ emu/cm$^3$, which safely discards interfacial and/or substrate contributions to the ferromagnetism. This value of $M_s$ compares well with the estimation of the concentration of $V_{Mg}$ in our samples by HRTEM. In addition, as shown in the lower inset of Fig. 3, films are colorless, shiny, and highly transparent making it possible to use them also for magneto-optical applications.

To further probe the predictions of our calculations regarding the spin polarization of the $2p$ O band we have performed XMCD and x-ray resonant magnetic scattering (XRMS) experiments at the 7 T high-field end station in the UE46-PGM1 beamline, at BESSY II. Both techniques are element selective and have therefore been used to rule out magnetism due to parasitic magnetic impurities as well as to demonstrate that it originates on oxygen ions. Thus absorption and reflection spectra at the Fe and Ni $L_{3,2}$ edges as well as at the O and Mg $K$ edges were measured simultaneously for right ($R^+$) and left ($R^-$) helicities of polarized incident radiation. Noteworthy, with these techniques Nefedov *et al.*[43] recently measured 1% XMCD asymmetry in reflection geometry $AR = (R^+ - R^-)/(R^+ + R^-)$ at the O $K$ edge ($1s \rightarrow 2p$) in the case of Co-doped $TiO_2$ for which a FM spin polarization of up to 0.06 $\mu_B$ was predicted. In our case, the reflection spectra as well as the XMCD asymmetry measured at the O $K$ edge in MgO samples are depicted in Fig. 4. We observed a clear magnetic spectrum at the O $K$ edge. We surmise that this XRMS asymmetry indicates that the room-temperature ferromagnetism of MgO films originates at O atoms. Note that the observed XRMS asymmetry probes the projection of the orbital polarization of the unoccupied $2p$ states of oxygen. This by itself does not guarantees that the oxygen $2p$ states are at the origin of the magnetization since a polarization of the unoccupied $2p$ states might be induced by the hybridization of the oxygen with $3d$ bands from a transition-metal cation.[44] Nevertheless we can safely exclude this possibility in the present case because traces of $3d$ impurities were not detected either by means of XMCD or by XRMS. In addition, the hybridization of the O $2p$ shell with the $3d$ orbitals of transition metals leads to sharp dichroic contributions around 530 eV. In our case, the nonzero XRMS asymmetry is observed for a broad energy range, excluding therefore any $3d$-metal doping contribution to the magnetic moment observed within the oxygen. We conclude the nonzero difference spectra, with a maximum AR of 4% at 535.2 eV, reveal a difference between spin populations of the oxygen sublattice due to cation vacancies, thus confirming the intrinsic origin of the magnetism observed in our samples.

## IV. DISCUSSION AND CONCLUSIONS

The origin of magnetism in undoped MgO is a topic of much recent interest. Some authors[45] claimed that magnetism in MgO is a surface phenomenon that cannot be sustained in bulk, even though theoretical results indicate that spin polarization may appear at the top of the valence band when Mg vacancies are introduced. However, our experimental results clearly evidence that magnetism can be sustained in MgO thin films up to room temperature (see Figs. 3 and 4). As we have shown, the local magnetic moments arise from the spin polarization of $2p$ orbitals of oxygen atoms nearest to Mg vacancies, in agreement with previous results. The observed XMCD signal at the O $K$ edges clearly supports the intrinsic nature of the observed ferromagnetism in MgO films. Noteworthy, high-resolution electron microscopy images are consistent with the presence of cation vacancies within the MgO matrix (a rough estimation give values of the $V_{Mg}$ density close to $2V_{Mg}/\text{nm}^3$) in our MgO thin films. Moreover, the theoretical expected magnetization value is in good agreement with the experiment, thus indicating that a successful description has been achieved.

Liu *et al.*[46] have investigated the electronic properties of MgO doped with elements such as B, Al, Ga, C, Ge, Si, and N. It is found that for the dopant atoms replacing oxygen in MgO, the system exhibits half-metallic ferromagnetic properties, although the metal-doped MgO films would be difficult to synthesize because of their large formation energies. These limitations could be avoided by metal-atom substitution for the Mg in MgO (beyond the scope of this paper). Preliminary results for extended calculations anticipate magnetization values above 500 emu/cm$^3$ when Mn substitutes Mg.

Regarding to the interactions mediating the ferromagnetism we cannot give a definitive answer from our experimental results. Two different scenarios can be envisaged. The local moments, mainly confined to the O atoms and their nearest neighbors, would lead to room-temperature ferromagnetism in the itinerant limit via a double exchange-like coupling within the impurity band. However, in the more

realistic localized limit the coupling must be due to direct exchange local impurity state overlap, as already shown in Ref. 47. In this regard, Stoneham[48] mentioned that the admixture of states from two *V* centers 2 nm apart each other might provide a long-range interaction. As noted above, our experimental and calculated results give a vacancy-vacancy distance about 1 nm. Still, carrier localization has been shown to control the washing out of ferromagnetism in a system such as Mn-doped GaAs,[19] though recent evidences showed that a strong ferromagnetic coupling between Mn exists before the emergence of fully itinerant hole carries.[49] Obviously further work is required before firm conclusions can be drawn.

Yet our findings have strong implications both from an applied and a fundamental point of view. They warrant a lively discussion regarding the role of defects in transforming insulating nonmagnetic materials into ferromagnets and might facilitate its application in future spin-based devices. Noteworthy, a number of phenomena which occur in conventional MgO-based magnetic tunnel junctions may be related to the effects we have been discussing.[50] For instance, our results suggest a differently spin-dependent confinement of electrons in the spacer layer, in support of recent experimental observations on interlayer exchange coupling across MgO spacers with different oxygen contents.[51]

Moreover, the properties we have described are probably significant in several devices of current and future technological importance. In this way, the artificial introduction of vacancies can be used as an effective method to tune the resistance-area product in spin-transfer torque core elements of future magnetic random access memories. On the other hand, the effects induced in the optical spectra by the cation vacancies anticipate visible emission luminescence in MgO thin films occurring simultaneously with the development of vacancy-induced magnetism.[52] In this regard, further work is needed to understand the nature and mobility of the hole polarons bound to Mg vacancies, and how changes in the defect density and, for instance, hydroxide passivation, affect the magnetic output and thermal stability.[53,54] Finally, when the hole is localized onto one, rather than all six of the oxygen atoms adjacent to the cation vacancy, it has been shown there is a big gain of polarization energy.[48] Since the hole can gain in kinetic energy by spreading out on all the surrounding oxygen atoms, it is envisaged the *V* centers could be aligned by an electric field, accompanied by a *p*-type semiconductivity.[24] For that reason, voltage-controlled switching phenomena are also expected in a metal-oxide-metal structure comprising Mg-defective MgO.[55,56]

## ACKNOWLEDGMENTS

We gratefully acknowledge financial support from the Spanish MICINN (Grant No. MAT2009-08024) and Consolider-Ingenio Program (Grant No. CSD2007-00041). Z. Konstantinović and C. Martínez-Boubeta are supported through the *Ramón y Cajal* program. We also thank A. Cebollada and V. Martínez for the careful reading of the manuscript.

*ben.martinez@icmab.es

[1] T. Dietl and H. Ono, MRS Bull. **28**, 714 (2003).
[2] N. H. Hong, J. Sakai, N. Poirot, and V. Brizé, Phys. Rev. B **73**, 132404 (2006).
[3] A. K. Rumaiz, B. Ali, A. Ceylan, M. Boggs, T. Beebe, and S. I. Shah, Solid State Commun. **144**, 334 (2007).
[4] A. Sundaresan, R. Bhargavi, N. Rangarajan, U. Siddesh, and C. N. R. Rao, Phys. Rev. B **74**, 161306(R) (2006).
[5] M. Li, S. Ge, W. Qiao, L. Zhang, Y. Zuo, and S. Yan, Appl. Phys. Lett. **94**, 152511 (2009).
[6] Y. Liu, Z. Lockman, A. Aziz, and J. MacManus-Driscoll, J. Phys.: Condens. Matter **20**, 165201 (2008).
[7] J. Červenka, M. I. Katsnelson, and C. F. J. Flipse, Nat. Phys. **5**, 840 (2009).
[8] Z. H. Zhang, X. Wang, J. B. Xu, S. Muller, C. Ronning, and Q. Li, Nat. Nanotechnol. **4**, 523 (2009).
[9] P. Larson and S. Satpathy, Phys. Rev. B **76**, 245205 (2007).
[10] F. Gao, J. Hu, C. Yang, Y. Zheng, H. Qin, L. Sun, X. Kong, and M. Jiang, Solid State Commun. **149**, 855 (2009).
[11] H. Peng, H. J. Xiang, S.-H. Wei, S.-S. Li, J.-B. Xia, and J. Li, Phys. Rev. Lett. **102**, 017201 (2009).
[12] H. Ohno, Science **281**, 951 (1998).
[13] A. Droghetti, C. D. Pemmaraju, and S. Sanvito, Phys. Rev. B **78**, 140404(R) (2008).
[14] P. Dev, Y. Xue, and P. Zhang, Phys. Rev. Lett. **100**, 117204 (2008).
[15] J. A. Chan, S. Lany, and A. Zunger, Phys. Rev. Lett. **103**, 016404 (2009).
[16] L. E. Halliburton, D. L. Cowan, W. B. J. Blake, and J. E. Wertz, Phys. Rev. B **8**, 1610 (1973).
[17] E. H. Izen, R. M. Mazo, and J. C. Kemp, J. Phys. Chem. Solids **34**, 1431 (1973).
[18] A. M. Ferrari and G. Pacchioni, J. Phys. Chem. **99**, 17010 (1995).
[19] M. Sawicki, D. Chiba, A. Korbecka, Y. Nishitani, J. A. Majewski, F. Matsukura, T. Dietl, and H. Ohno, Nat. Phys. **6**, 22 (2010).
[20] K. P. McKenna and A. L. Shluger, Phys. Rev. B **79**, 224116 (2009).
[21] K. Oumi, H. Matsumoto, K. Kashiwagi, and Y. Murayama, Surf. Coat. Technol. **169-170**, 562 (2003).
[22] T. F. Dossin, M.-F. Reyniers, R. J. Berger, and G. B. Marin, Appl. Catal., B **67**, 136 (2006).
[23] Y. Chen, W. A. Sibley, F. D. Srygley, R. A. Weeks, E. B. Hensley, and R. L. Kroes, J. Phys. Chem. Solids **29**, 863 (1968).
[24] M. M. Freund, F. Freund, and F. Batllo, Phys. Rev. Lett. **63**, 2096 (1989).
[25] H. S. Jung, J.-K. Lee, M. Nastasi, S.-W. Lee, J.-Y. Kim, J.-S. Park, K. S. Hong, and H. Shin, Langmuir **21**, 10332 (2005).
[26] T. Uchino and D. Okutsu, Phys. Rev. Lett. **101**, 117401 (2008).
[27] M. Bowen, V. Cross, F. Petroff, A. Fert, C. Martínez-Boubeta, J. L. Costa-Krämer, J. V. Anguita, A. Cebollada, F. Briones, J. M.

de Teresa, L. Morellón, R. Ibarra, F. Güell, F. Peirò, and A. Cornet, Appl. Phys. Lett. **79**, 1655 (2001).
[28] A. Schmehl, V. Vaithyanathan, A. Herrnberger, S. Thiel, C. Richter, M. Liberati, T. Heeg, M. Röckerath, L. F. Kourkoutis, S. Mühlbauer, P. Böni, D. A. Muller, Y. Barash, J. Schubert, Y. Idzerda, J. Mannhart, and D. G. Schlom, Nature Mater. **6**, 882 (2007).
[29] J. Goniakowski and C. Noguera, Phys. Rev. B **60**, 16120 (1999).
[30] B. Gu, N. Bulut, T. Ziman, and S. Maekawa, Phys. Rev. B **79**, 024407 (2009).
[31] S. Gallego, J. I. Beltran, J. Cerda, and M. C. Munoz, J. Phys.: Condens. Matter **17**, L451 (2005).
[32] J. I. Beltrán and C. Monty, Ll. Balcells, and C. Martínez-Boubeta, Solid State Commun. **149**, 1654 (2009).
[33] P. Ordejón, E. Artacho, and J. M. Soler, Phys. Rev. B **53**, R10441 (1996).
[34] J. P. Perdew, K. Burke, and M. Ernzerhof, Phys. Rev. Lett. **77**, 3865 (1996).
[35] I. S. Elfimov, S. Yunoki, and G. A. Sawatzky, Phys. Rev. Lett. **89**, 216403 (2002).
[36] J. I. Beltrán, M. C. Muñoz, and J. Hafner, New J. Phys. **10**, 063031 (2008).
[37] S. A. Chambers, T. T. Tran, and T. A. Hileman, J. Mater. Res. **9**, 2944 (1994).
[38] D. Peterka, C. Tegenkamp, K.-M. Schröder, W. Ernst, and H. Pfnür, Surf. Sci. **431**, 146 (1999).
[39] C. Martinez-Boubeta, Z. Konstantinović, Ll. Balcells, S. Estradé, J. Arbiol, A. Cebollada, and B. Martínez, Cryst. Growth Des. **10**, 1017 (2010).
[40] J. Arbiol, S. Estradé, J. D. Prades, A. Cirera, F. Furtmayr, C. Stark, A. Laufer, M. Stutzmann, M. Eickhoff, M. H. Gass, A. L. Bleloch, F. Peiró, and J. R. Morante, Nanotechnology **20**, 145704 (2009).
[41] H. K. Yu, W.-K. Kim, J.-L. Lee, E. C. Park, J. S. Kim, and J. H. Ryu, Jpn. J. Appl. Phys. **48**, 076003 (2009).
[42] R. González, M. A. Monge, J. E. Muñoz Santiuste, R. Pareja, Y. Chen, E. Kotomin, M. M. Kuklja, and A. Popov, Phys. Rev. B **59**, 4786 (1999).
[43] A. Nefedov, N. Akdogan, H. Zabel, R. I. Khaibullin, and L. R. Tagirov, Appl. Phys. Lett. **89**, 182509 (2006).
[44] C. Sorg, N. Ponpandian, M. Bernien, K. Baberschke, H. Wende, and R. Q. Wu, Phys. Rev. B **73**, 064409 (2006).
[45] F. Wang, Z. Pang, L. Lin, S. Fang, Y. Dai, and S. Han, Phys. Rev. B **80**, 144424 (2009).
[46] G. Liu, S. Ji, L. Yin, G. Fei, and C. Ye, J. Phys.: Condens. Matter **22**, 046002 (2010).
[47] V. Pardo and W. E. Pickett, Phys. Rev. B **78**, 134427 (2008).
[48] M. Stoneham, J. Phys.: Condens. Matter **22**, 074211 (2010).
[49] S. R. Dunsiger, J. P. Carlo, T. Goko, G. Nieuwenhuys, T. Prokscha, A. Suter, E. Morenzoni, D. Chiba, Y. Nishitani, T. Tanikawa, F. Matsukura, H. Ohno, J. Ohe, S. Maekawa, and Y. J. Uemura, Nature Mater. **9**, 299 (2010).
[50] R. Stearrett, W. G. Wang, L. R. Shah, A. Gokce, J. Q. Xiao, and E. R. Nowak, J. Appl. Phys. **107**, 064502 (2010).
[51] Y. F. Chiang, J. J. I. Wong, X. Tan, Y. Li, K. Pi, W. H. Wang, H. W. K. Tom, and R. K. Kawakami, Phys. Rev. B **79**, 184410 (2009).
[52] W. C. Las and T. G. Stoebe, Radiat. Prot. Dosim. **8**, 45 (1984).
[53] M. M. Abraham, Y. Chen, and W. P. Unruh, Phys. Rev. B **9**, 1842 (1974).
[54] A. Gibson, R. Haydock, and J. P. LaFemina, Phys. Rev. B **50**, 2582 (1994).
[55] G. Dearnaley, A. M. Stoneham, and D. V. Morgan, Rep. Prog. Phys. **33**, 1129 (1970).
[56] P. Krzysteczko, G. Reiss, and A. Thomas, Appl. Phys. Lett. **95**, 112508 (2009).